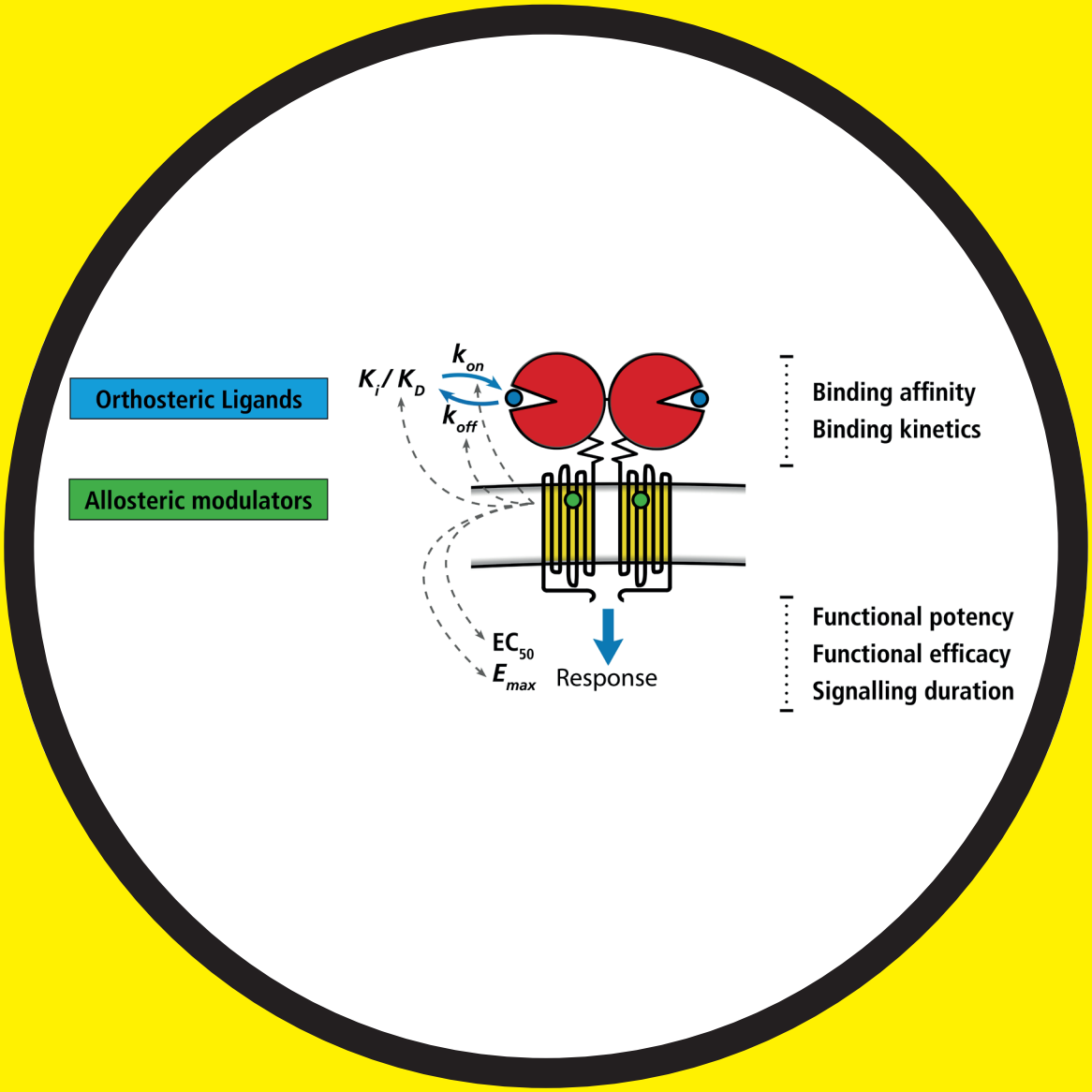
Orthosteric Ligands
Allosteric modulators
K_i / K_D
k_{on}
k_{off}
EC_{50}
E_{max}
Response
Binding affinity
Binding kinetics
Functional potency
Functional efficacy
Signalling duration

CHAPTER 3

Impact of allosteric modulation: Exploring the binding kinetics of glutamate and other orthosteric ligands of the metabotropic glutamate receptor 2

Maarten L J Doornbos, Sophie C Vermond, Hilde Lavreysen, Gary Tresadern, Adriaan P IJzerman & Laura H Heitman

Biochemical Pharmacology 155 (2018) 356–365. doi:10.1016/j.bcp.2018.07.014

3

ABSTRACT

While many orthosteric ligands have been developed for the $mGlu_2$ receptor, little is known about their target binding kinetics and how these relate to those of the endogenous agonist glutamate. Here, the kinetic rate constants, i.e. k_{on} and k_{off}, of glutamate were determined for the first time followed by those of the synthetic agonist LY354740 and antagonist LY341495. To increase the understanding of the binding mechanism and impact of allosteric modulation thereon, kinetic experiments were repeated in the presence of allosteric modulators. Functional assays were performed to further study the interplay between the orthosteric and allosteric binding sites, including an impedance-based morphology assay.

We found that dissociation rate constants of orthosteric $mGlu_2$ ligands were all within a small 6-fold range, whereas association rate constants were ranging over more than three orders of magnitude and correlated to both affinity and potency. The latter showed that target engagement of orthosteric $mGlu_2$ ligands is k_{on}-driven *in vitro*. Moreover, only the off-rates of the two agonists were decreased by a positive allosteric modulator (PAM), thereby increasing their affinity. Interestingly, a PAM increased the duration of a glutamate-induced cellular response. A negative allosteric modulator (NAM) increased both on- and off-rate of glutamate without changing its affinity, while it did not affect these parameters for LY354740, indicating probe-dependency.

In conclusion, we found that affinity- or potency-based orthosteric ligand optimization primarily results in ligands with high k_{on} values. Moreover, positive allosteric modulators alter the binding kinetics of orthosteric agonists mainly by decreasing k_{off}, which we were able to correlate to a lengthened cellular response. Together, this study shows the importance of studying binding kinetics in early drug discovery, as this may provide important insights towards improved efficacy *in vivo*.

INTRODUCTION

Glutamate is the most important excitatory neurotransmitter in the central nervous system where it modulates synaptic responses via activation of ionotropic glutamate receptors and metabotropic glutamate (mGlu) receptors.[1] mGlu receptors are class C G protein-coupled receptors (GPCRs) that structurally consist of a large extracellular glutamate binding domain, the so-called Venus Flytrap (VFT) domain, which is connected via a cysteine-rich domain to the typical seven-transmembrane (7TM) domain.[2] The $mGlu_2$ receptor, which is expressed presynaptically in the periphery of the synapse, is of interest in drug discovery as it negatively modulates the release of glutamate into the synapse.[3] Hence, $mGlu_2$ receptor activation can reduce glutamate hyperfunction in diseases like schizophrenia and anxiety,[4,5] whereas $mGlu_2$ receptor blockade can be beneficial for glutamate hypofunction in depression and impaired cognition.[6,7]

A variety of glutamate-like ligands targeting the orthosteric binding site in the VFT domain was developed including the reference agonist LY354740 and antagonist LY341495.[8,9] Until the recent disclosure of the $mGlu_2$ selective agonist LY2812223,[10] development of orthosteric ligands presented challenges for receptor subtype selectivity and therefore discovery efforts shifted to allosteric modulators that bind in a less conserved pocket in the 7TM domain.[11] Allosteric modulators enhance or inhibit the potency and/or efficacy of the endogenous/orthosteric agonist with little or no intrinsic activity.[12] . Two positive allosteric modulators (PAMs) have advanced into clinical trials: AZD8529[13,14] and JNJ-40411813/ADX71149.[15,16] Reference PAMs in the field include BINA[17], JNJ-40068782[18] and JNJ-46281222.[19] A number of negative allosteric modulators (NAMs) have been characterized *in vivo*, including a recent series of Janssen, RO4491533 and decoglurant of which the latter has advanced into clinical trials.[7,20–22]

Over the last decade it has become increasingly clear that *in vivo* efficacy is not only depending on optimized *in vitro* affinity and efficacy parameters, but also on optimized kinetics of both receptor binding and activation.[23] The dissociation rate constant k_{off} and its derived parameter residence time (RT = $1/k_{off}$) have received increasing attention since the *in vivo* efficacy of multiple marketed GPCR drugs was shown to be related to long RT at the target, such as the long-acting M_3 receptor antagonist tiotropium.[24,25] Although most kinetic studies have emphasized dissociation rate constants, association rate constants have also been described to be important for fast onset of drug action, a high receptor occupancy and even a longer duration of action.[26,27] The importance of k_{on} was further underscored for its potential in drug safety by Sykes *et al.* (2017) who showed that extrapyramidal side effects induced by dopamine D_2 receptor antagonists are linked to k_{on} rather than k_{off} as had been the general hypothesis so far.[28]

We have recently shown the importance of k_{on} and k_{off} for $mGlu_2$ PAMs, where their affinity was k_{on}-driven and their k_{off} was linked to *in vivo* efficacy, as shown in **Chapter 4**.[29] Except for this study, no previous studies have extensively focused on binding kinetics of $mGlu_2$ ligands. Understanding of binding kinetics may also be helpful in drug discovery of novel orthosteric $mGlu_2$ ligands. Moreover, appreciating the kinetic binding parameters of the endogenous agonist is important when designing orthosteric ligands as they have to compete for the same binding site.[30] Furthermore, determination of alterations of the kinetic parameters of the endogenous ligand induced by an allosteric modulator will provide valuable mechanistic insights. Since kinetic binding parameters of the endogenous $mGlu_2$ agonist glutamate have not been quantified before we set up a kinetic radioligand binding assay to enable quantification of kinetic parameters for orthosteric ligands. The major mechanism of action of many allosteric modulators is to modulate endogenous agonist affinity by affecting its kinetic binding parameters, as affinity is determined by $K_D = k_{off} / k_{on}$. Therefore, kinetic binding experiments with orthosteric ligands were also performed in the presence of a PAM or NAM. Additionally, we performed functional assays, i.e. [^{35}S]GTPγS binding assays measuring G protein activation and a label-free biosensor assay that measures changes in cell morphology representing a more integral cellular response. These functional assays were used to further study the interplay between the orthosteric and allosteric binding sites, and its effect on the level of functional efficacy. Importantly, the cell morphology assay enabled recording in real-time, thereby providing the opportunity to evaluate functional receptor-induced responses over time in addition to the time-dependent binding kinetics assays.

This work provides insights on the binding kinetics of orthosteric ligands at the $mGlu_2$ receptor and modulation thereof by PAMs or NAMs. As such, it contributes to increased molecular understanding which may strengthen future drug discovery projects focusing on the development of both orthosteric ligands or allosteric modulators for the $mGlu_2$ receptor as well as for other GPCRs.

MATERIALS AND METHODS

Chemicals and Reagents

LY354740, JNJ-46281222, JNJ-40068782, BINA, RO4491533, and [^{3}H]JNJ-46281222 were synthesized at Janssen Research and Development. LY341495 was from Tocris BioScience (Bristol, UK). [^{3}H]LY341495 was obtained from American Radiolabeled Companies (St. Louis, MO, USA) and [^{35}S]GTPγS from PerkinElmer (Groningen, The Netherlands). Dulbecco's modified Eagle's medium (DMEM), glutamate, GDP and Glutamate-pyruvate transaminase (GPT) were from Sigma Aldrich (St. Louis, MO, USA). Penicillin, streptomycin, L-Proline and

G418 were obtained from Duchefa Biochemie (Haarlem, The Netherlands). Fetal calf serum (FCS) was from Biowest (Nuaillé, France). CHO-K1 cells stably expressing the wildtype (WT) $hmGlu_2$ receptor (CHO-K1_$hmGlu_2$) were from Janssen Research and Development. Other chemicals were from standard commercial sources.

Cell culture

CHO-K1_$hmGlu_2$ cells were cultured in Dulbecco's modified Eagle's medium (DMEM) supplemented with 10% (v/v) fetal calf serum, 200 IU·mL^{-1} penicillin, 200 μg·mL^{-1} streptomycin, 30.5 μg·mL^{-1} L-proline and 400 μg·mL^{-1} G418 at 37°C and 5% CO_2. Cells were subcultured twice every week at a ratio of 1:10.

Membrane preparation

Membrane preparation was performed as in **Chapter 2**.

Radioligand binding assays

[^{3}H]LY341495 binding assays

Membranes were thawed and subsequently homogenized using an Ultra Turrax homogenizer at 24,000 rpm (IKA-Werke GmbH & Co.KG, Staufen, Germany). Assay buffer (50 mM Tris-HCl pH 7.4, 2 mM $CaCl_2$, 10 mM $MgCl_2$) was used to dilute the samples to a total reaction volume of 100 μl containing 5 μg membrane protein and 4 nM [^{3}H]LY341495. Incubations were performed at 0°C. Nonspecific binding was determined using 1 mM glutamate and DMSO concentrations were ≤0.25%.

Displacement experiments were carried out using radioligand and a competing ligand at multiple concentrations. Samples were incubated for 60 minutes, after which receptor-bound radioactivity was determined.

Association experiments were performed by incubation of radioligand in the absence or presence of allosteric modulator at 1 μM with membrane aliquots. The amount of receptor-bound radioligand was determined at different time points up to 60 minutes.

Dissociation experiments were carried out by a 60 minute pre-incubation of radioligand and membrane aliquots in the absence or presence of allosteric modulator at 1 μM. The amount of receptor-bound radioligand was determined after dissociation at different time points up to 60 minutes which was initiated by addition of 5 μl assay buffer containing LY341495 (final concentration 10 μM).

Competition association experiments were performed by incubation of radioligand, competing ligand at its IC_{50} concentration in the absence or presence of allosteric modulator at 1 μM with membrane aliquots. The amount of receptor-bound radioligand was determined at different time points up to 60 minutes.

For all assays, incubations were terminated by rapid filtration over GF/C filter plates (PerkinElmer) using a PerkinElmer 96w Filtermate harvester. Subsequently filters were

washed five times using ice-cold wash buffer (50 mM Tris-HCl pH 7.4). Filter-bound reactivity was determined using liquid scintillation spectrometry on a Microbeta 2450[2] microplate counter (PerkinElmer).

[^{3}H]JNJ-46281222 binding assays

Experiments were performed as described under '[^{3}H]LY341495 binding assays' with the following alterations: [^{3}H]JNJ-46281222 was used at 6 nM, membrane aliquots contained 30 μg, incubations were performed at 15°C and non-specific binding was determined using 10 μM JNJ-40068782. Incubations were terminated by rapid filtration over Whatman GF/C filters (GE Healthcare Life Sciences, Buckinghamshire, UK) on a Brandel harvester 24 (Brandel, Gaithersburg, MD, USA). Filters were washed three times with ice-cold wash buffer (50 mM Tris-HCl pH 7.4). Filter-bound reactivity was determined using a TriCarb 2810 TR counter (PerkinElmer).

[^{35}S]GTPγS binding assays

Membrane homogenates (10 μg) were diluted in assay buffer (50 mM Tris-HCl pH 7.4, 100 mM NaCl, 3 mM $MgCl_2$) supplemented with 5 μg saponin and 10 μM GDP to a total volume of 80 μl containing increasing concentrations of ligand of interest in the absence or presence of a glutamate concentration equivalent to its EC_{80} value (60 μM), if indicated. Basal and maximal receptor activity was determined in the presence of only assay buffer or 1 mM glutamate, respectively. After a 30 minute pre-incubation at 25°C, 20 μl [^{35}S]GTPγS (final concentration 0.3 nM) was added. Reactions were stopped after 90 minutes incubation at 25°C. Filtration was performed and filter-bound radioactivity determined as described under '[^{3}H]LY341495 binding assays' except that GF/B filter plates were used and the wash-buffer consisted of 50 mM TRIS-HCl and 5 mM $MgCl_2$.

Impedance-based morphology assays

Impedance-based morphology assays were performed using the real-time cell analyser (RTCA) xCELLigence SP system (ACEA Biosciences, San Diego, CA, USA),[31,32] as previously described.[33] The system measures electrical impedance generated by adherence of cells to gold-coated electrodes at the bottom of 96 wells PET E-plates (obtained from Bioké, Leiden, the Netherlands). Changes in impedance (Z) are measured continuously and are displayed as Cell Index (CI), which is defined as $(Z_i - Z_0)\ \Omega / 15\Omega$. Z_i is the impedance at a given time and Z_0 is the baseline impedance measured at the start of the experiment in the absence of cells. Baseline impedance was determined using 45 μl culture medium (as described under 'cell culture') per well in a 96 well E-plate. 40,000 CHO-K1_hmGlu$_2$ cells were added in a volume of 50 μl per well. After resting at room temperature for 30 minutes, the plate was mounted in the recording station within a humidified 37°C, 5% CO_2 incubator. Impedance was measured every 15 minutes overnight. 18 hours after cell seeding, wells were stimulated with increasing concentrations of glutamate in the absence or presence of 1 μM PAM JNJ-46281222, resulting in final well volumes of 100 μl. DMSO concentrations were 0.025% and constant between wells.

Data analysis

Data analyses were performed using Prism 7.00 (GraphPad software, San Diego, CA, USA). pIC_{50} values in radioligand displacement assays were obtained by non-linear regression curve fitting into a sigmoidal concentration-response curve using the equation: Y=Bottom + (Top-Bottom)/(1+10$^{(X-LogIC50)}$). pK_i values were obtained from pIC_{50} values using the Cheng-Prusoff equation.[34] Dissociation rate constant k_{off} was obtained using an exponential decay analysis of radioligand binding. Association rate constant k_{on} was determined using the equation $k_{on} = (k_{obs} - k_{off})/[L]$, in which L is the concentration of radioligand and k_{obs} was determined using an exponential association analysis of radioligand binding.

Association and dissociation rate constants for unlabelled $mGlu_2$ PAMs were determined by nonlinear regression analysis of competition association data as described by Motulsky and Mahan.[35]

$$K_A = k_1[L]\cdot 10^{-9} + k_2$$
$$K_B = k_3[I]\cdot 10^{-9} + k_4$$
$$S = \sqrt{(K_A - K_B)^2 + 4\cdot k_1 \cdot k_3 \cdot L \cdot I \cdot 10^{-18}}$$
$$K_F = 0.5(K_A + K_B + S)$$
$$K_S = 0.5(K_A + K_B - S)$$
$$Q = \frac{B_{\max}\cdot k_1 \cdot L \cdot 10^{-9}}{K_F - K_S}$$
$$Y = Q\cdot\left(\frac{k_4\cdot(K_F - K_S)}{K_F \cdot K_S} + \frac{k_4 - K_F}{K_F}e^{(-K_F\cdot X)} - \frac{k_4 - K_S}{K_S}e^{(-K_S\cdot X)}\right)$$

pEC_{50} and pIC_{50} values in the [^{35}S]GTPγS binding assays were determined using non-linear regression curve fitting into a sigmoidal concentration-response curve using the equation: Y=Bottom + (Top-Bottom)/(1+10^($LogEC_{50}$-X)*Hill Slope)). The same equation was used to determine pEC_{50} values from the impedance-based morphology assay. Baseline-corrected ΔCI levels at indicated time points were used to obtain these concentration-response curves. Data are shown as mean ± SEM of at least three individual experiments performed in duplicate. Statistical analyses were performed as indicated. If p-values were below 0.05, observed differences were considered statistically significant.

RESULTS

Affinity of orthosteric compounds in the absence or presence of allosteric modulators

The affinities of orthosteric agonists glutamate and LY354740 and antagonist LY341495 were determined by [^{3}H]LY341495 displacement assays in the absence and presence of PAMs JNJ-46281222 (1 μM), BINA (10 μM) and JNJ-40068782 (1 μM) or NAM RO4491533 (1 μM)

(Fig. 1A-C, Table 1). The affinity of both the endogenous agonist glutamate and the synthetic agonist LY354740 was significantly increased in the presence of all PAMs. Specifically, in presence of JNJ-46281222, glutamate affinity was increased by 7-fold (pK_i 4.52 ± 0.04 to 5.40 ± 0.08 in the absence and presence of JNJ-46281222, respectively), while the affinity of LY354740 was increased by 5-fold (pK_i 6.79 ± 0.01 to 7.51 ± 0.15 in the absence and presence of JNJ-46281222, respectively). The affinity of antagonist LY341495 (pK_i 8.39 ± 0.09) was not affected by any of the PAMs. The presence of 1 μM NAM RO4491533 did not affect the affinity of glutamate, LY354740 or LY341495, which shows that the presence of the NAM does not inhibit the orthosteric agonists and antagonist from binding to the receptor. Since JNJ-46281222 induced the highest shift in agonist affinity it was used as representative PAM for further experimentation, along with RO4491533 as a representative NAM. Of note, both JNJ-46281222 and RO4491533 were not able to displace the radiolabelled orthosteric antagonist [^{3}H]LY341495 by themselves (Fig. 1D), which indicates that they bind to an allosteric site at the $mGlu_2$ receptor.

Figure 1. Effect of allosteric modulators on the affinity of orthosteric ligands. [^{3}H]LY341495 displacement by orthosteric agonists A) glutamate and B) LY354740 and antagonist C) LY341495 in

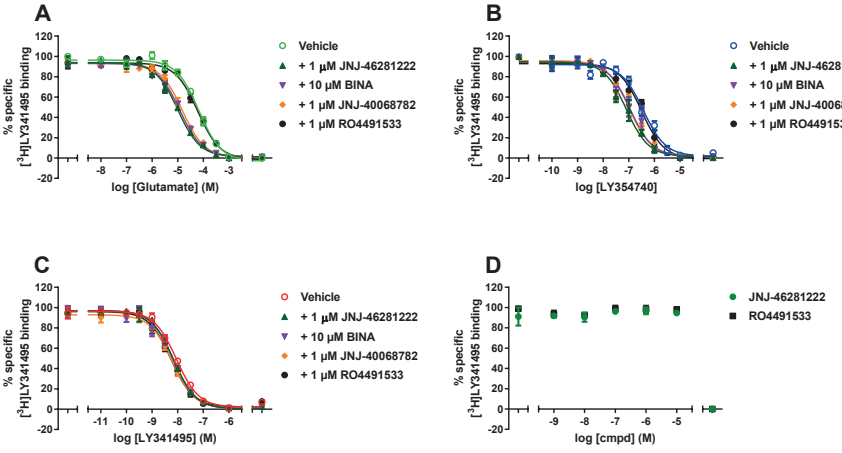

the absence or presence of PAMs or NAM. D) [^{3}H]LY341495 binding in the presence of increasing concentrations of the PAM JNJ-46281222 or NAM RO4491533. Data represent the mean ± SEM of three individual experiments performed in duplicate. If not shown, error bars are within the symbol.

Table 1. Affinity (pK_i) of orthosteric ligands in the absence and presence of allosteric modulators determined in [^{3}H]LY341495 displacement assays.

	Glutamate	LY354740	LY341495
Vehicle	4.52 ± 0.04	6.79 ± 0.01	8.39 ± 0.09
+ *1 μM JNJ-46281222*	5.40 ± 0.08***	7.51 ± 0.15*	8.54 ± 0.02
+ *10 μM BINA*	5.30 ± 0.09***	7.38 ± 0.03*	8.57 ± 0.08
+ *1 μM JNJ-40068782*	5.23 ± 0.04***	7.43 ± 0.19*	8.59 ± 0.05
+ *1 μM RO4491533*	4.56 ± 0.03	6.93 ± 0.15	8.65 ± 0.10

Values represent the mean ± SEM of three individual experiments performed in duplicate. Statistical analyses were performed using a one-way ANOVA with Dunnett's post-test. * < 0.05, *** < 0.001.

Binding kinetics of orthosteric compounds

We set-up radioligand binding assays allowing the determination of binding kinetics of orthosteric compounds in the absence or presence of allosteric modulators. The kinetic binding parameters k_{on} and k_{off} of [^{3}H]LY341495 were determined using classical (direct) association and dissociation assays (Fig. 2A, Table 2). [^{3}H]LY341495 associated rapidly to the mGlu$_2$ receptor, where complete association was reached within 5 minutes, resulting in a k_{obs} value of 0.015 ± 0.0007 s^{-1}. Dissociation induced by 10 µM unlabelled LY341495 yielded a k_{off} value of 0.0066 ± 0.0001 s^{-1}. Based on these k_{obs} and k_{off} values and the concentration of the radioligand used, k_{on} was calculated as 2.2 ± 0.17 x 10^6 M^{-1} s^{-1}. To obtain kinetic binding parameters for unlabelled orthosteric compounds, a competition association assay was performed (Fig. 2B-D). The assay was first validated using unlabelled LY341495, for which k_{on} and k_{off} values were comparable to those obtained in the classical association and dissociation assays (Table 2). Subsequently, the kinetic binding parameters of glutamate and LY354740 were assessed (Fig. 2C,D; Table 3). Compared to LY341495, glutamate had a significantly lower k_{on} value of 1.6 ± 0.3 x 10^3 M^{-1}s^{-1} and a faster dissociation rate (k_{off} 0.036 ± 0.008 s^{-1}). Interestingly, LY354740 had a k_{off} value similar to that of glutamate, but a 40-fold higher k_{on} value (k_{off} 0.045 ± 0.010 min^{-1} and k_{on} 7.1 ± 2.9 x 10^4 M^{-1}s^{-1}, respectively). Of note, the K_D values, i.e. calculated based on their k_{on} and k_{off} values, for glutamate, LY35470 and LY341495, were in good agreement with the K_i values obtained from equilibrium displacement assays (compare Tables 1 and 3).

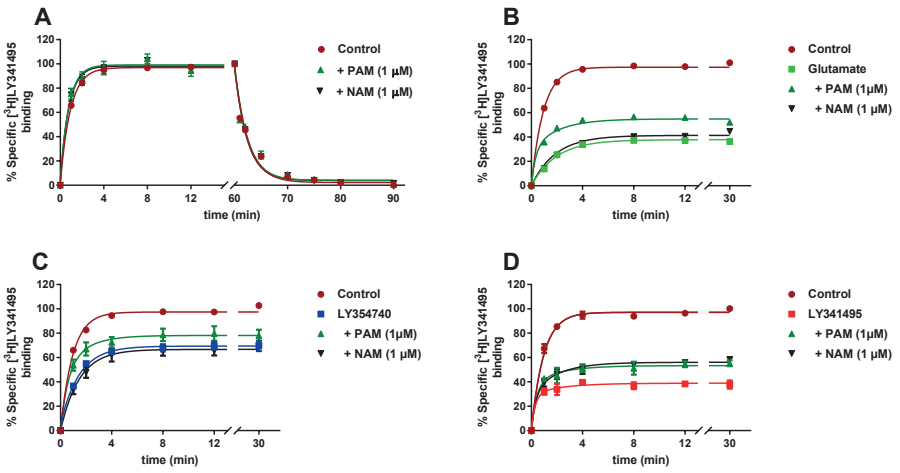

Figure 2. Binding kinetics of orthosteric ligands and the effects of allosteric modulators thereon. A) Association and dissociation kinetics of 4 nM [^{3}H]LY341495 at the mGlu$_2$ receptor at 0°C in the absence or presence of PAM JNJ-46281222 or NAM RO4491533 at 1 µM. Competition association of the agonists B) glutamate and C) LY354740 and D) antagonist LY341495 in the absence or presence of PAM JNJ-46281222 or NAM RO4491533 at 1 µM. Data represent the mean ± SEM of at least three individual experiments performed in duplicate.

Table 2. Comparison of kinetic binding parameters (k_{on}, k_{off}) antagonist LY341495 in the absence or presence of JNJ-46281222 (PAM) or RO4491533 (NAM), determined by direct [3H]LY341495 association and dissociation assays.

	K_D (nM)[a]	k_{on} (M^{-1} s^{-1})	k_{off} (s^{-1})
LY341495	2.9 ± 0.23	(2.2 ± 0.17) x 10^6	0.0066 ± 0.0001
+ *1 μM PAM*	2.9 ± 0.24	(2.2 ± 0.67) x 10^6	0.0063 ± 0.0003
+ *1 μM NAM*	3.2 ± 0.17	(2.1 ± 0.65) x 10^6	0.0068 ± 0.0002

[a] Kinetic K_D values, defined by $K_D = k_{off} / k_{on}$. Values represent the mean ± SEM of three individual experiments performed in duplicate.

Table 3. Kinetic binding parameters (k_{on}, k_{off}) for agonists glutamate and LY354740 and antagonist LY341495 in the absence or presence of JNJ-46281222 (PAM) or RO4491533 (NAM) obtained from competition association assays using [^{3}H]LY341495.

	K_D (nM)[a] (pK_D)	k_{on} (M^{-1} s^{-1})	k_{off} (s^{-1})
Glutamate	23000 ± 6900 (4.65)	(1.6 ± 0.3) x 10^3	0.036 ± 0.008
+ *1 μM PAM*	4700 ± 600* (5.33)	(2.4 ± 0.18) x 10^3	0.012 ± 0.001*
+ *1 μM NAM*	23500 ± 2400 (4.63)	(5.2 ± 0.37) x 10^3***	0.12 ± 0.009***
LY354740	630 ± 290 (6.20)	(7.1 ± 2.9) x 10^4	0.045 ± 0.010
+ *1 μM PAM*	180 ± 20 (6.74)	(7.3 ± 0.56) x 10^4	0.013 ± 0.001*
+ *1 μM NAM*	550 ± 200 (6.26)	(8.5 ± 2.1) x 10^4	0.047 ± 0.013
LY341495	3.5 ± 0.46 (8.45)	(2.4 ± 0.18) x 10^6	0.0087 ± 0.0009
+ *1 μM PAM*	2.8 ± 0.40 (8.56)	(3.5 ± 0.46) x 10^6	0.0096 ± 0.0006
+ *1 μM NAM*	3.4 ± 1.2 (8.46)	(3.9 ± 0.93) x 10^6	0.013 ± 0.003

[a] Kinetic K_D values, defined by $K_D = k_{off} / k_{on}$. Values represent the mean ± SEM of three individual experiments performed in duplicate. Statistical analyses were performed using a one-way ANOVA with Dunnett's post-test. * < 0.05, ** < 0.01, *** < 0.001.

The effect of allosteric modulators on the binding kinetics of orthosteric compounds

The kinetic binding parameters k_{on} and k_{off} of glutamate, LY354740 and LY341495 were determined in the presence of PAM JNJ-46281222 or NAM RO4491533 at 1 μM (Fig. 2B-D; Table 3). The k_{on} value for glutamate in the presence of 1 μM JNJ-46281222 was slightly but not significantly increased to 2.4 ± 0.18 x 10^3 $M^{-1}s^{-1}$ compared to its value obtained in the absence of PAM. The k_{off} value on the other hand was significantly decreased by 3-fold to 0.012 ± 0.001 min^{-1}. Together, this resulted in an approximately 5-fold increased 'kinetic' affinity (K_D) for glutamate from 23 ± 6.9 to 4.7 ± 0.6 μM, which was also observed in the equilibrium displacement assays (K_i values, compare Tables 1 and 3). In the presence of 1 μM RO4491533, the k_{on} value of glutamate was significantly increased by 3-fold to 5.2 ± 0.37 x 10^3 $M^{-1}s^{-1}$, while the k_{off} value was also significantly increased by 3-fold to 0.12 ± 0.009 s^{-1}. As a result, the kinetic K_D value did not change compared to glutamate in the absence of NAM (24 ± 2.4 μM and 23 ± 6.9 μM in absence or presence of NAM, respectively).

The k_{on} value of LY354740 was left unchanged in the presence of 1 μM JNJ-46281222 (7.3 ± 0.56 x 10^4 $M^{-1}s^{-1}$), whereas the k_{off} value was decreased by 3-fold to 0.013 ± 0.001 s^{-1}. Together

this led to an increased kinetic K_D value of 180 ± 20 nM of the agonist LY354740 in the presence of PAM JNJ-46281222. Interestingly, in contrast to glutamate, no significant shifts in k_{on} or k_{off} values were seen for the agonist LY354740 in the presence of 1 μM RO4491533, and therefore the kinetic K_D was also unaffected (630 ± 290 and 550 ± 200 nM in absence or presence of NAM, respectively). Lastly, both k_{on} and k_{off} values of the antagonist LY341495 were not significantly altered by the presence of PAM or NAM. This was the case for both the direct [^{3}H]LY341495 association and dissociation assays (Fig. 2A, Table 2), as well as for the competition association assays (Fig. 2D, Table 3). Hence, K_D values were similar to those obtained in the absence of allosteric modulator.

Potency and efficacy of orthosteric ligands, effects of allosteric modulators on LY354740 potency and efficacy

To evaluate the effects of JNJ-46281222 and RO4491533 on the functional responses induced by orthosteric compounds, a functional [^{35}S]GTPγS binding assay was used that measures compound-induced G protein activation. Firstly, concentration-response curves of the agonists glutamate and LY354740 were made (Fig. 3A), which led to pEC_{50} values of 4.95 ± 0.01 and 6.94 ± 0.04, respectively. The maximum level of [^{35}S]GTPγS binding induced by the synthetic agonist LY354740 was 83.5 ± 1.2% compared to the maximum response induced by the endogenous agonist glutamate (100% at 1 mM) (Table 4). The potency of the antagonist LY341495 was determined in the presence of an EC_{80} concentration of glutamate (60 μM). LY341495 inhibited glutamate-induced [^{35}S]GTPγS binding with a pIC_{50} value of 7.40 ± 0.04 (Fig. 3A). Secondly, the effects of increasing concentrations of JNJ-46281222 or RO4491533 on the concentration-response curves of LY354740 were assessed (Fig. 3B, Table 4). Increasing concentrations of the PAM JNJ-46281222 induced a concentration-dependent increase in E_{max} up to approximately 220% at a concentration of 30 nM or higher. Moreover, the potency of LY354740 was increased significantly from 6.94 ± 0.04 in the absence of PAM to 7.69 ± 0.07 in the presence of 100 nM JNJ-46281222. In contrast, when LY35470 was treated with increasing concentrations of the NAM RO4491533, the E_{max} values of the concentration-response curves were reduced concentration-dependently. At a concentration of 30 nM RO4491533 or higher, LY354740-induced [^{35}S]GTPγS binding was completely abolished (Fig. 3C, Table 4). Interestingly, the potency of LY354740 did not change significantly in the presence of increasing NAM concentrations.

Effect of PAM JNJ-46281222 on duration of glutamate-induced cellular response using an impedance-based morphology assay

To gain further insights in the functional impact of allosteric modulation, receptor activation by glutamate was evaluated using an impedance-based morphology assay (i.e. xCELLigence). This method can record receptor-specific cellular responses in real-time, and thus compound-induced changes in cellular dynamics can be measured over time.

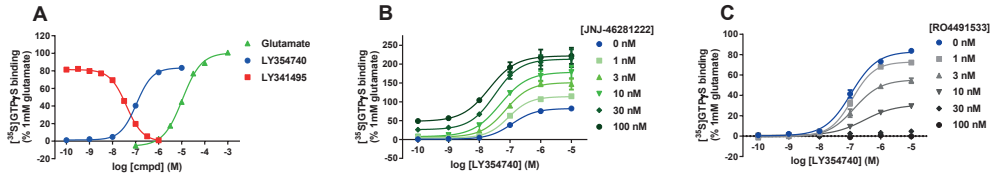

Figure 3. Effect of allosteric modulators on intrinsic agonist potency and efficacy. A) Concentration-response curves of glutamate- and LY354740-induced [^{35}S]GTP**γ**S binding and concentration-response curve of inhibition of glutamate induced (EC_{80}: 60μM) [^{35}S]GTP**γ**S binding by LY341495. Effects of increasing concentrations of B) JNJ-46281222 and C) RO4491533 on concentration-response curves of LY354740 in the [^{35}S]GTP**γ**S binding assay. Data are expressed as the percentage of maximal response induced by 1 mM glutamate (100%) and represent the mean ± SEM of three individual experiments performed in duplicate. If not shown, error bars are within the symbol.

Table 4. Effect of allosteric modulators JNJ-46281222 (PAM) and RO4491533 (NAM) on LY354740-induced [^{35}S]GTPγS binding.

	pEC_{50}	E_{max} (%)[a]
LY354740	6.94 ± 0.04	83.5 ± 1.2
+ *1 nM JNJ-46281222*	7.04 ± 0.10	117 ± 4.2
+ *3 nM JNJ-46281222*	7.14 ± 0.08	154 ± 11**
+ *10 nM JNJ-46281222*	7.35 ± 0.10**	178 ± 16***
+ *30 nM JNJ-46281222*	7.50 ± 0.07****	215 ± 22****
+ *100 nM JNJ-46281222*	7.69 ± 0.07****	222 ± 22****
+ *1 nM RO4491533*	6.91 ± 0.07	74.5 ± 1.3**
+ *3 nM RO4491533*	6.87 ± 0.11	55.5 ± 2.5****
+ *10 nM RO4491533*	6.69 ± 0.05	30.0 ± 1.6****

[a] Expressed as percentage of [^{35}S]GTPγS binding induced by 1 mM glutamate (set at 100%). Values represent the mean ± SEM of three individual experiments performed in duplicate. Statistical analyses were performed using a one-way ANOVA with Dunnett's post-test. ** < 0.01, *** < 0.001, **** < 0.0001.

Glutamate-induced responses were recorded at increasing concentrations in the absence and presence of 1 μM PAM JNJ-46281222 resulting in a concentration-dependent increase in impedance, depicted as Cell Index (Fig.4A,B). Similar to the [^{35}S]GTPγS assay, the glutamate potency was significantly ($p < 0.05$, student's t-test) increased from pEC_{50} 5.27 ± 0.19 to 5.99 ± 0.12 in the absence and presence of PAM, respectively. Furthermore, the PAM-induced shift in potency for glutamate in the morphology assay was comparable to the shift for LY354740 in the [^{35}S]GTPγS assay (Table 4). Interestingly, the duration of the glutamate-induced response in the presence of PAM was also increased from approximately 45 to over 60 minutes. To further evaluate this effect, concentration-response curves of glutamate in the absence and presence of the PAM were obtained at two different time points after stimulation, i.e. 15 and 45 minutes (Fig. 4C,D). Comparison of these concentration-response curves yielded a 2-fold decrease in efficacy for the curve from the later time point (Fig. 4C), congruent with the almost loss of glutamate signal in the absence of PAM at 45 minutes (Fig. 4A). In contrast, the

glutamate efficacy in the presence of PAM did not change significantly, when comparing the concentration-response curves of 15 and 45 minutes after stimulation. This is in line with the observation that the duration of the glutamate-induced response is prolonged by the PAM to approximately 60 minutes, and thus a decrease in cellular impedance was not yet observed at 45 minutes (Fig. 4B). Of note, when comparing the potencies for each condition, i.e. glutamate in the absence or presence of PAM, these were not significantly different at the two time points selected (Fig. 4C,D).

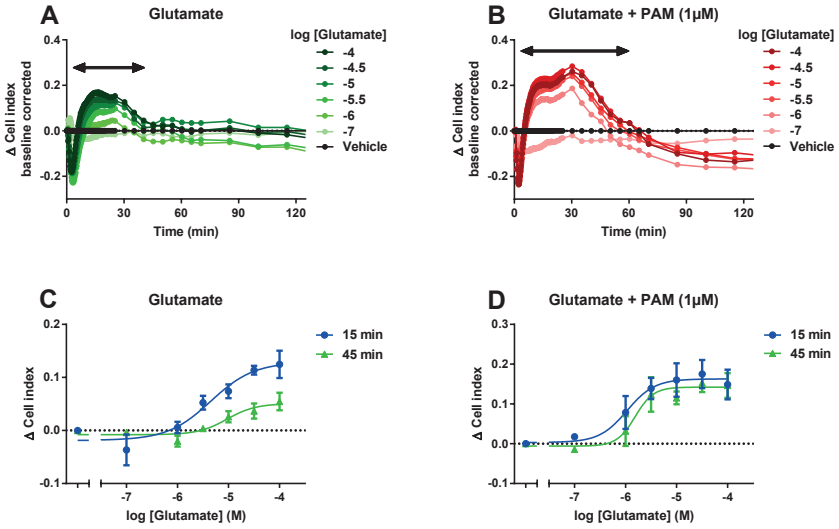

Figure 4. Effect of PAM JNJ-46281222 on the duration of glutamate-induced signalling, as determined by an impedance-based morphology assay. A,B) 18 hours after seeding, CHO-K1_hmGlu$_2$ cells (40,000 cells/well) were stimulated by increasing concentrations of the agonist glutamate in absence (A) or presence of 1 μM of the PAM JNJ-46281222 (B). Medium with 0.025% DMSO was used as vehicle control. DMSO concentrations were 0.025% in all cases. A representative example is shown of a baseline-corrected response, the so-called Δ cell index (ΔCI), which was repeated at least three times in duplicate. C,D) Concentration-response curves were obtained from the ΔCI values at 15 or 45 minutes after stimulation. pEC$_{50}$ values are mentioned in the results section. xCELLigence traces (A, B) are from a representative experiment. Curves (C, D) represent mean ± SEM of at least three individual experiments performed in duplicate.

Correlations and kinetic map

To compare the parameters obtained from the different radioligand binding assays, correlation plots were made (Fig. 5A-C). As mentioned above, the affinity values obtained from [^{3}H]LY341495 equilibrium displacement assays (K_i) and [^{3}H]LY341495 competition association assays (K_D) were in very good agreement, as exemplified by a high linear correlation (Fig. 5A, R^2 = 0.95), further corroborating the robustness of the latter assay. A significant correlation was also found between affinity (K_i) and association rate constants (k_{on}) (Fig. 5B, R^2 = 0.99). Such a correlation, however, was not found between affinity (K_i) and dissociation rate

constants (k_{off}) (Fig. 5C, $R^2 = 0.29$), indicating that affinities of these orthosteric compounds are predominantly k_{on}-driven.

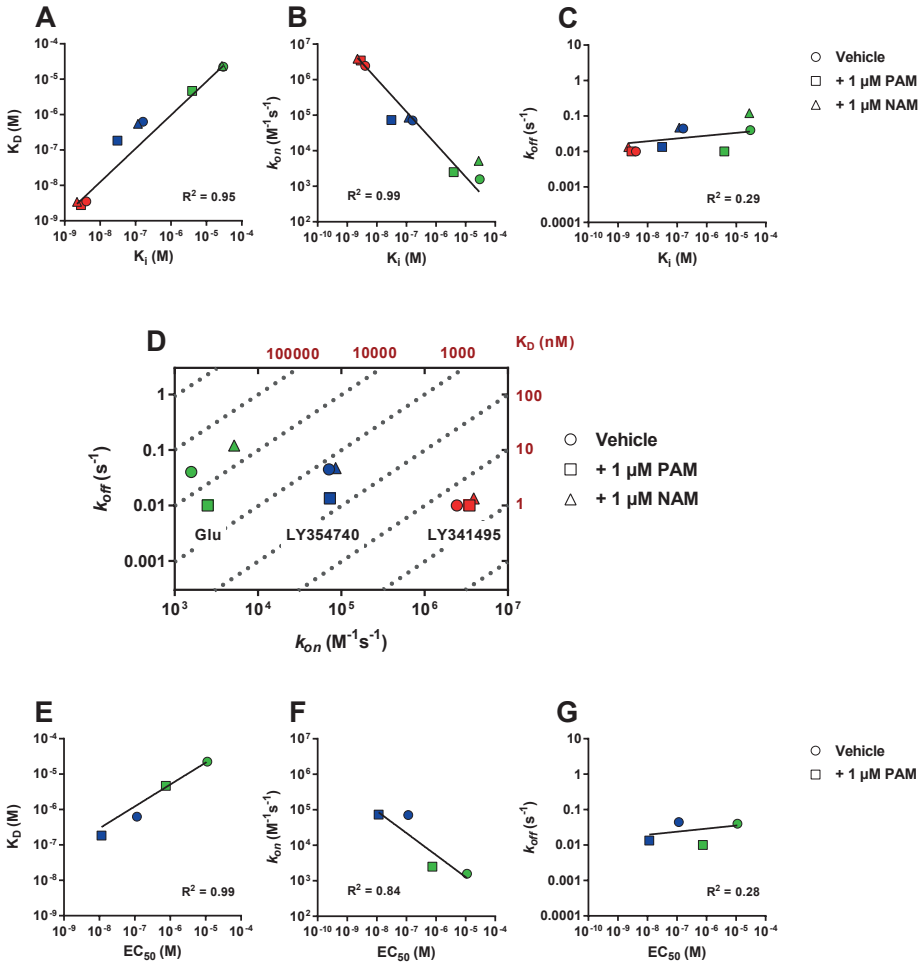

Figure 5. Correlations between affinity, potency and kinetic parameters. A,B,C) Correlation between affinity of glutamate (green), LY354740 (blue) and LY341495 (red) determined in [^{3}H]LY341495 equilibrium displacement assays (K_i) and affinity determined based on kinetic parameters k_{on} and k_{off} obtained from [^{3}H]LY341495 competition association assays (K_D) (A); affinity (K_i) and association rate constant (k_{on}) (B); affinity (K_i) and dissociation rate constant (k_{off}) (C). D) Kinetic map with the association rate constant (k_{on}) plotted on the x-axis and the dissociation rate constant (k_{off}) on the y-axis. Identical affinity (K_D) values may result from different combinations of k_{on} and k_{off} ($K_D = k_{off} / k_{on}$, diagonal dashed lines). E,F,G) Correlation between potency of glutamate and LY354740 determined in [^{35}S]GPTγS assays (EC_{50}) and affinity determined based on kinetic parameters k_{on} and k_{off} obtained from [^{3}H]LY341495 competition association assays (K_D) (E). The EC_{50} of glutamate in the presence of 1 µM PAM is from [19]; potency (EC_{50}) and association rate constant (k_{on}) (F); potency (EC_{50}) and dissociation rate constant (k_{off}) (G).

A kinetic map was made, to further compare the kinetic and affinity parameters (Fig. 5D). In this map k_{on} (x-axis), k_{off} (y-axis) and K_D (diagonal lines) values were plotted. k_{on} and K_D values ranged over more than three orders of magnitude, whereas k_{off} values were only spread within a single order of magnitude and therefore appeared at a similar horizontal level in the kinetic map (Fig. 5D).

As shown in Table 3, k_{on} and k_{off} values of glutamate were affected by both PAM and NAM, which was exemplified in the kinetic map by a spread in symbols. Specifically, in the presence of PAM, the k_{off} of glutamate was decreased by 3-fold. In the presence of NAM both k_{on} and k_{off} were increased 3-fold resulting in the same affinity as illustrated by a diagonal shift of the NAM symbol, i.e. a shift along the line of similar K_D. In the presence of PAM, the k_{off} of LY354740 was similarly affected compared to glutamate, i.e. in both cases this resulted in a downward shift on the kinetic map, whereas in the presence of NAM no significant shifts were observed, resulting in nearly overlapping symbols. Since the k_{on} and k_{off} values of LY34195 were not affected by PAM or NAM all three symbols are overlapping in the kinetic map.

To compare the functional potency of agonists in the absence or presence of PAM to the kinetic parameters k_{on} and k_{off} further correlation plots were made (Fig. 5E-G). Firstly, the potencies (EC_{50}) obtained in [^{35}S]GTPγS assays of agonists glutamate and LY354740 were shown to be strongly correlated (Fig. 5E, $R^2 = 0.99$) to the affinity obtained from competition association assays (K_D), showing that potencies are driven by the agonist binding affinities although the absolute values differed by approximately one log unit. As the affinities were shown to be correlated to on-rates, a correlation was also found between agonist potencies and k_{on} values (Fig. 5F, $R^2 = 0.84$), showing that a high agonist potency is obtained from a high on-rate. No correlation was found between agonist potency and dissociation rate constant (k_{off}) (Fig. 5G, $R^2 = 0.28$). However, in the presence of PAM the agonist k_{off} was decreased for both glutamate and LY354740, which then was the driver for an increased agonist potency, as was also observed for agonist affinity in the presence of PAM.

DISCUSSION

Traditionally, affinity and potency are the main parameters studied in *in vitro* drug discovery. In addition, a ligand's target binding kinetic parameters are nowadays commonly appreciated as valuable information for the early phases of drug discovery.[25] For the development of novel and effective orthosteric $mGlu_2$ ligands it is valuable to know their kinetic binding parameters, but also to understand how these relate to the binding kinetics of the endogenous agonist glutamate.[30] Moreover, a variety of high affinity and selective PAMs and

NAMs have been developed that modulate glutamate potency, efficacy and/or affinity. As for orthosteric compounds, it is equally useful to know the allosteric modulator's binding kinetics, as was shown in **Chapter 4**. Likewise it is also relevant to know how a modulator affects the kinetic binding parameters of the endogenous ligand glutamate. Hence, in the present study we aimed to increase the understanding of binding kinetics of orthosteric $mGlu_2$ ligands both on their own and upon modulation by an allosteric ligand.

The orthosteric ligands used in this study were the endogenous agonist glutamate and reference orthostertic ligands LY354740 (agonist) and LY341495 (antagonist). Radioligand displacement experiments (Fig.1, Table 1) showed that these ligands bind the same orthosteric binding site, which is in line with previous observations.[2,4] The kinetic parameters k_{on} and k_{off} of glutamate were quantified for the first time, using competition association experiments. To allow the set-up of this assay kinetic [^{3}H]LY341495 binding experiments were performed which showed that this ligand associates to its binding site within four minutes and dissociates in approximately ten minutes (Fig. 2A). For the set-up of the competition association assay, the association and dissociation of the radioligand should ideally be slower allowing more data points on the steep part of the curves.[36] This is often achieved by a temperature reduction. However, in these assays the temperature could not be lowered, since it had to be set at 0°C already to allow quantification of kinetic measurements using this commercially available radioligand. Still we could produce robust data between the different binding assays indicating their validity. To obtain values for kon and koff of unlabelled ligands in the absence and presence of allosteric modulators, the Motulsky and Mahan model was used [35,38]. This model requires input for the values of k_{on} and k_{off} (k_1 and k_2 in the model) of the labelled radioligand (i.e. [^{3}H]LY341495). Importantly, these values should remain constant throughout the experiments, as was the case here for [^{3}H]LY341495 which provided similar values for k_{on} and k_{off} both in the absence and presence of allosteric modulators (Table 2). Due to the nature of the radioligand (i.e. fast receptor association) there is not much resolution in the association phase of the curves, making it difficult to observe differences in the rates by eye. However, by analysis of the data with the Motulsky and Mahan model we were able to obtain robust binding kinetic parameters between different experiments.[35,36]

We found that glutamate dissociation (0.036 s^{-1}, Table 3) is fast in comparison to the series of $mGlu_2$ PAMs we studied in **Chapter 4**, which dissociate on a minute-range at 28°C (k_{off} values between 0.00033 and 0.0040 s^{-1}), which would be even slower at 0°C. The observation of fast glutamate binding kinetics is in line with studies using FRET sensors that found $mGlu_1$ receptor conformational changes upon glutamate binding within seconds.[37,38] Fast receptor dissociation of glutamate relates to its physiological role as a neurotransmitter, where short bursts of glutamate at high concentrations are released into the synapse where it should evoke its function during that burst only.[3] Similarly, fast off-rates were obtained for other

endogenous neurotransmitters as exemplified by 2-AG and anandamide on the CB_2 receptor (k_{off} = 0.053 s^{-1} and 0.012 s^{-1} at 25°C, respectively)[39] and acetylcholine on the M_3 receptor (k_{off} = 0.093 s^{-1} at 37°C).[40] Comparison of these values is troublesome, since for practical reasons experiments were performed at different temperatures. Still, they all share off-rates on the second to minute scale, indicating fast receptor dissociation particularly when comparing to synthetic ligands at the same receptors.[39,40]

It is generally acknowledged that allosteric modulators may change the affinity and/or potency of agonists by modulating their k_{on} and/or k_{off} values.[41] Generally this has been determined by radioligand dissociation experiments in the presence of allosteric modulators that enable quantification of modulated off-rates.[42] Limitations of such assays are that it is impossible to detect effects on a radioligand's on-rate and that the orthosteric/endogenous ligand of interest needs to be radiolabelled. This is not suitable for most endogenous agonists including glutamate due to a too low target affinity, or too high non-specific binding. Therefore, we used the competition association assay for quantification of both k_{on} and k_{off} values of unlabelled orthosteric ligands in the absence or presence of PAM or NAM, as was recently published for an adenosine A_1 receptor PAM.[36] The presence of PAM JNJ-46281222 at 1 μM significantly reduced the k_{off} of glutamate and LY354740, resulting in an increased affinity for both these agonists. This was in line with the results from the radioligand displacement assay (Table 1) and can be considered a typical PAM effect.[41] A similar effect was also seen in the functional [^{35}S]GTPγS binding assay where the potency of LY354740 was increased by the PAM JNJ-46281222 by almost 6-fold and its efficacy was more than doubled in line with the results obtained using glutamate in **Chapter 2**. Furthermore, a decreased k_{off}, i.e. increased residence time, for glutamate in the presence of 1 μM PAM JNJ-46281222 results in a prolonged receptor occupancy, which correlated to a prolonged cellular response in the morphology assay (Fig. 4). This functional assay is performed on whole cells under physiologically more relevant conditions (i.e. in culture medium, at 37°C, in a CO_2 incubator) and is therefore considered to be more translational than classical functional assays.[31,32]

Furthermore, the assay can be performed in real-time, which enabled translation from kinetic binding parameters towards functional efficacy over time. Previous studies have also used this assay to study the link between receptor binding kinetics, functional activation kinetics and duration of signalling for agonist-induced responses on the dopamine D_2 and neurokinin 1 receptors.[43,44] Of note, we have shown in **Chapter 6** that culture medium contains 100 μM endogenous glutamate,[45] and therefore the enzyme glutamate-pyruvate transaminase (GPT) is often used to reduce this level. In the current study we were interested in the effect of a PAM on glutamate-responses, as this is the endogenous ligand and thus most relevant for PAM drug discovery. Therefore, GPT could not be used as this would deplete exogenous glutamate in addition to endogenous glutamate.

The NAM RO4491533 at 1 μM positively modulated both k_{on} and k_{off} of glutamate (Table 3), resulting in an unchanged affinity. Of note, these effects on glutamate kinetics cannot be observed in the classical radioligand displacement assays at equilibrium conditions, and would therefore be missed (Table 1). On the other hand, RO4491533 was not able to change k_{on} and k_{off} of LY354740, which shows that the effects of this NAM on binding kinetics of agonists were probe-dependent.[12] This finding highlights the importance of using endogenous agonists in studies of allosteric modulation, since results on other (synthetic) agonists may provide different conclusions as a result of probe-dependency. The observation that a high 1 μM concentration of NAM RO4491533 did not modulate the affinity of both agonists indicated that these ligands still bind the orthosteric binding site in the presence of this NAM, which is therefore behaving as a silent or neutral allosteric ligand (NAL) concerning orthosteric ligand binding.[11] On the contrary, RO4491533 displayed a strong negative cooperativity in the functional [^{35}S]GTPγS binding assay as it concentration-dependently decreased the efficacy of the agonist LY354740 without changing its potency, eventually resulting in abolished LY354740 efficacy (Fig. 3; Table 4), similar to its effects on glutamate activity.[22] This mode of negative allosteric modulation, i.e. only affecting efficacy, has been found across the class C GPCR family. NAMs such as CPCCOEt ($mGlu_1$) and MPEP ($mGlu_5$) also abolished agonist efficacy without modulation of binding affinity.[46,47] The absence of cooperativity between LY341495 and both PAM and NAM was further illustrated by the observation that k_{on} and k_{off} of LY341495 were not affected by any allosteric modulator (Table 3).

The kinetic parameters of glutamate, LY354740 and LY341495 were most different in k_{on}, ranging over more than three orders of magnitude (from 1.6 ± 0.3 x 10^3 to 2.4 ± 0.18 x 10^6 $M^{-1}min^{-1}$) as did their affinity values, whereas k_{off} values were all within a 6-fold range (from 0.0087 ± 0.0009 to 0.045 ± 0.010). The correlation plots figure 5 show that k_{on} is strongly correlated to the agonist affinity and potency, which indicates that target engagement of orthosteric $mGlu_2$ ligands is k_{on}-driven. Recent simulation studies have emphasized the role of high k_{on} values for receptor occupancy and drug dosing.[26,27] A mechanism responsible for these effects may be receptor rebinding, which is described as the binding of newly dissociated ligand from the local environment of the receptor.[48] The interstitial localization of the $mGlu_2$ receptor may result in more rebinding due to less diffusion and therefore higher local concentrations. However, rebinding to the $mGlu_2$ receptor seems less likely for glutamate due to its low k_{on} value (both in the absence and presence of a PAM – Table 3) and the active lowering of local glutamate concentrations by glutamate transporters expressed on the neuronal cell membrane and surrounding glial cells.[49] In contrast, rebinding may play a more prominent role in binding of synthetic ligands which have higher k_{on} values and are not actively transported away from their site of action, resulting in higher *in vivo* receptor occupancy.[48] The plots in figure 5 furthermore showed that whereas between different PAMs a higher affinity is obtained from a higher k_{on}, the higher agonist affinity and potency obtained in the presence

of a PAM results from a lowered k_{off} value as has been shown to be a common mechanism of action for many PAMs at different GPCRs.[41] As shown in figure 5, k_{off} is not correlated to both affinity and potency. This is similar to our recent work on $mGlu_2$ PAMs presented in **Chapter 4** and this may therefore be a receptor-specific property. Furthermore, this earlier study provided a first indication that PAM k_{off} values may be correlated to *in vivo* efficacy, as measured by effects on sleep-wake architecture in rats, more specifically suppression of Rapid Eye Movement (REM) sleep.[50] In the light of the current observation that the presence of a PAM prolonged glutamate-induced cellular responses by decreasing its k_{off}, it may be speculated that k_{off} values of both the PAM and the endogenous agonist are important for the duration of action and thus also for *in vivo* efficacy. As such, this information is valuable for the design of novel orthosteric and allosteric ligands in early drug discovery.

CONCLUSION

In conclusion, the set-up of a competition association radioligand binding assay enabled quantification of the parameters of binding kinetics for glutamate for the first time. k_{off} values of the orthosteric compounds were within a single order of magnitude, whereas k_{on} values were spread over more than three orders of magnitude and were strongly correlated to affinity, indicating that $mGlu_2$ target engagement is driven by k_{on} rather than k_{off}. Binding kinetics of agonists were modulated by the PAM, showing a decrease in k_{off} of both agonists and a prolonged functional response for glutamate. The NAM altered k_{on} and k_{off} of glutamate without changing glutamate's affinity, but did not induce such alterations for agonist LY354740, which indicates probe-dependency. These results show that affinity or potency-only optimization of orthosteric ligands will result in a high k_{on} value but not necessarily optimized k_{off} values, which is essential for optimal *in vivo* efficacy, as shown by previous studies. Together, this work contributes to an increased understanding of the molecular processes that underlie the mechanism of GPCR allosteric modulation, specifically how allosteric modulators affect the kinetic parameters of the endogenous agonist. Therefore, this study further emphasizes the need for evaluation of binding kinetics during drug discovery of both orthosteric and allosteric drug candidates for the $mGlu_2$ receptor as well as for other GPCRs.

REFERENCES

1. Kew JNC, Kemp JA. *Psychopharmacology (Berl)*. **2005**; 179: 4–29.

2. Pin J-P, Duvoisin R. *Neuropharmacology*. **1995**; 34: 1–26.

3. Nicoletti F, Bockaert J, Collingridge GL, Conn PJ, Ferraguti F, Schoepp DD, Wroblewski JT, Pin JP. *Neuropharmacology*. **2011**; 60: 1017–41.

4. Dunayevich E, Erickson J, Levine L, Landbloom R, Schoepp DD, Tollefson GD. *Neuropsychopharmacology*. **2008**; 33: 1603–10.

5. Patil ST, Zhang L, Martenyi F, Lowe SL, Jackson KA, Andreev B V, Avedisova AS, Bardenstein LM, Gurovich IY, Morozova MA, Mosolov SN, Neznanov NG, Reznik AM, Smulevich AB, Tochilov VA, Johnson BG, Monn JA, Schoepp DD. *Nat Med*. **2007**; 13: 1102–7.

6. Feyissa AM, Woolverton WL, Miguel-Hidalgo JJ, Wang Z, Kyle PB, Hasler G, Stockmeier CA, Iyo AH, Karolewicz B. *Prog Neuropsychopharmacol Biol Psychiatry*. **2010**; 34: 279–83.

7. Goeldner C, Ballard TM, Knoflach F, Wichmann J, Gatti S, Umbricht D. *Neuropharmacology*. **2013**; 64: 337–46.

8. Kingston A., Ornstein P., Wright R., Johnson B., Mayne N., Burnett J., Belagaje R, Wu S, Schoepp D. *Neuropharmacology*. **1998**; 37: 1–12.

9. Schaffhauser H, Richards JG, Cartmell J, Chaboz S, Kemp JA, Klingelschmidt A, Messer J, Stadler H, Woltering T, Mutel V. *Mol Pharmacol*. **1998**; 53: 228–33.

10. Monn JA, Prieto L, Taboada L, Hao J, Reinhard MR, Henry SS, Beadle CD, Walton L, Man T, Rudyk H, Clark B, Tupper D, Baker SR, Lamas C, Montero C, Marcos A, Blanco J, Bures M, Clawson DK, Atwell S, Lu F, Wang J, Russell M, Heinz BA, Wang X, Carter JH, Getman BG, Catlow JT, Swanson S, Johnson BG, Shaw DB, McKinzie DL. *J Med Chem*. **2015**: 7526–48.

11. Conn PJ, Christopoulos A, Lindsley CW. *Nat Rev Drug Discov*. **2009**; 8: 41–54.

12. Keov P, Sexton PM, Christopoulos A. *Neuropharmacology*. **2011**; 60: 24–35.

13. Homepage: https://clinicaltrials.gov/show/NCT00986531. The Effects AZD8529 on Cognition and Negative Symptoms in Schizophrenics. (accessed April 12, 2018)

14. Homepage: https://clinicaltrials.gov/show/NCT02401022. The Study of AZD8529 for Smoking Cessation in Female Smokers. (accessed April 12, 2018)

15. Salih H, Anghelescu I, Kezic I, Sinha V, Hoeben E, Van Nueten L, De Smedt H, De Boer P. *J Psychopharmacol*. **2015**; 29: 414–425.

16. Kent JM, Daly E, Kezic I, Lane R, Lim P, De Smedt H, De Boer P, Van Nueten L, Drevets WC, Ceusters M. *Prog Neuro-Psychopharmacology Biol Psychiatry*. **2016**; 67: 66–73.

17. Galici R, Echemendia NG, Rodriguez AL, Conn PJ. *J Pharmacol Exp Ther*. **2005**; 315: 1181–7.

18. Lavreysen H, Langlois X, Ahnaou A, Drinkenburg W, te Riele P, Biesmans I, Van der Linden I, Peeters L, Megens A, Wintmolders C, Cid JM, Trabanco AA, Andrés JI, Dautzenberg FM, Lütjens R, Macdonald G, Atack JR. *J Pharmacol Exp Ther*. **2013**; 346: 514–27.

19. Doornbos MLJ, Pérez-Benito L, Tresadern G, Mulder-Krieger T, Biesmans I, Trabanco AA, Cid JM, Lavreysen H, IJzerman AP, Heitman LH. *Br J Pharmacol*. 2016; 173: 588–600.

20. Homepage: https://clinicaltrials.gov/show/NCT01457677. ARTDeCo Study: A study of RO4995819 in patients with major depressive disorder and inadequate response to ongoing antidepressant treatment. (Accessed April 12, 2018)

21. Van Gool M, Alonso De Diego SA, Delgado O, Trabanco AA, Jourdan F, Macdonald GJ, Somers M, Ver Donck L. *ChemMedChem*. **2017**; 12: 905–912.

22. Campo B, Kalinichev M, Lambeng N, El Yacoubi M, Royer-Urios I, Schneider M, Legrand C, Parron D, Girard F, Bessif A,

Poli S, Vaugeois J-M, Le Poul E, Celanire S. *J Neurogenet*. **2011**; 25: 152–66.

23. Swinney DC, Haubrich BA, Liefde I Van, Vauquelin G. *Curr Top Med Chem*. **2015**; 15: 2504–22.

24. Dowling MR, Charlton SJ. *Br J Pharmacol*. **2006**; 148: 927–37.

25. Copeland RA. *Nat Rev Drug Discov*. **2016**; 15: 87–95.

26. Vauquelin G. *Br J Pharmacol*. **2016**; 173: 2319–2334.

27. de Witte WEA, Danhof M, van der Graaf PH, de Lange ECM. *Trends Pharmacol Sci*. **2016**; 37: 831–842.

28. Sykes DA, Moore H, Stott L, Holliday N, Javitch JA, Lane JR, Charlton SJ. *Nat Commun*. **2017**; 8: 763.

29. Doornbos MLJ, Cid JM, Haubrich J, Nunes A, van de Sande JW, Vermond SC, Mulder-Krieger T, Trabanco AA, Ahnaou A, Drinkenburg WH, Lavreysen H, Heitman LH, IJzerman AP, Tresadern G. *J Med Chem*. **2017**; 60: 6704–6720.

30. Nederpelt I, Bleeker D, Tuijt B, IJzerman AP, Heitman LH. *Biochem Pharmacol*. **2016**; 118: 88–95.

31. Xi B, Yu N, Wang X, Xu X, Abassi YA. *Biotechnol J*. **2008**; 3: 484–495.

32. Yu N, Atienza JM, Bernard J, Blanc S, Zhu J, Wang X, Xu X, Abassi Y. *Anal Chem*. **2006**; 78: 35–43.

33. Hillger JM, Schoop J, Boomsma DI, Eline Slagboom P, IJzerman AP, Heitman LH. *Biosens Bioelectron*. **2015**; 74: 233–242.

34. Cheng Y, Prusoff WH. *Biochem Pharmacol*. **1973**; 22: 3099–108.

35. Motulsky HJ, Mahan LC. *Mol Pharmacol*. **1984**; 25: 1–9.

36. Guo D, Venhorst SN, Massink A, van Veldhoven JPD, Vauquelin G, IJzerman AP, Heitman LH. *Br J Pharmacol*. **2014**; 171: 5295–312.

37. Tateyama M, Abe H, Nakata H, Saito O, Kubo Y. *Nat Struct Mol Biol*. **2004**; 11: 637–42.

38. Hlavackova V, Zabel U, Frankova D, Bätz J, Hoffmann C, Prezeau L, Pin J-P, Blahos J, Lohse MJ. *Sci Signal*. **2012**; 5: ra59.

39. Martella A, Sijben H, Rufer A, Fingerle J, Grether U, Ullmer C, Hartung T, IJzerman A, van der Stelt M, Heitman L. *Mol Pharmacol*. **2017**: mol.117.108605.

40. Sykes DA, Dowling MR, Charlton SJ. *Mol Pharmacol*. **2009**; 76: 543–51.

41. Christopoulos A, Kenakin T. *Pharmacol Rev*. **2002**; 54: 323–74.

42. Lane JR, May LT, Parton RG, Sexton PM, Christopoulos A. *Nat Chem Biol*. **2017**; 13: 929–937.

43. Nederpelt I, Kuzikov M, de Witte WEA, Schnider P, Tuijt B, Gul S, IJzerman AP, de Lange ECM, Heitman LH. *Sci Rep*. **2017**; 7: 14169.

44. Klein Herenbrink C, Sykes DA, Donthamsetti P, Canals M, Coudrat T, Shonberg J, Scammells PJ, Capuano B, Sexton PM, Charlton SJ, Javitch JA, Christopoulos A, Lane JR. *Nat Commun*. **2016**; 7: 1–14.

45. Doornbos MLJ, Van der Linden I, Vereyken L, Tresadern G, IJzerman AP, Lavreysen H, Heitman LH. *Biochem Pharmacol*. **2018**; 152: 201–210.

46. Litschig S, Gasparini F, Rueegg D, Stoehr N, Flor PJ, Vranesic I, Prézeau L, Pin JP, Thomsen C, Kuhn R. *Mol Pharmacol*. **1999**; 55: 453–61.

47. Bradley SJ, Langmead CJ, Watson JM, Challiss RAJ. *Mol Pharmacol*. **2011**; 79: 874–85.

48. Vauquelin G, Charlton SJ. *Br J Pharmacol*. **2010**; 161: 488–508.

49. Marcaggi P, Attwell D. *Glia*. **2004**; 47: 217–225.

50. Ahnaou A, Lavreysen H, Tresadern G, Cid JM, Drinkenburg WH. *PLoS One*. **2015**; 10: e0144017.